Thermal Ionization Ideal Gas Chemical Equilibrium Calculations for Jupiter's Atmosphere

Professor Bruce Fegley, Jr.

Planetary Chemistry Laboratory (solarsystem.wustl.edu)

Department of Earth & Planetary Sciences and McDonnell Center for the Space Sciences,

Washington University, St Louis MO 63130 USA

Prepared 14 December 2017, Updated 5 June 2022

Please cite as B. Fegley, Jr., 2022. "Thermal ionization ideal gas chemical equilibrium calculations for Jupiter's atmosphere" Report 2022-1, Planetary Chemistry Laboratory (solarsystem.wustl.edu), Department of Earth & Planetary Sciences and McDonnell Center for the Space Sciences, Washington University, St Louis MO 63130 USA

Summary. The major conclusions from thermal ionization ideal gas calculations done along a model Jovian adiabatic P, T profile are as follows:

1. Electron sources –The major electron source is thermal ionization of elemental gases

(a) Hydrogen is the major electron source in the absence of alkali metals, which are removed from the overlying atmosphere by cloud condensation deep in Jupiter's atmosphere (Fegley & Lodders 1994, Lodders 1999). The net thermochemical reaction for ionization of monatomic hydrogen is

$$H = H^+ + e^-$$

(b) If present in the gas, i.e., deeper than the cloud base altitude level of condensation clouds incorporating most of these elements, potassium (1st) and sodium (2nd) are the dominant electron sources and their net thermochemical ionization reactions are

$$K = K^+ + e^-$$

$$Na = Na^+ + e^-$$

(c) Less important – Lithium (high IP and low abundance), rubidium and cesium (low IP but low abundance)

2. Electron sources – Via chemical equilibria forming protonated cations

$$H_2 + H^+ = H_3^+$$

$$NH_3 + H^+ = NH_4^+$$

$$H_2O + H^+ = H_3O^+(hydronium)$$

Formation of protonated cations, like those shown above, depletes the H^+ abundance, leading to further ionization of monatomic H to maintain a constant value for the reaction quotient at a given temperature. This is a demonstration of LeChatelier's Principle and is described in chapter 10 of Fegley (2013).

3. Electron sinks – Via electron attachment reactions forming anions

$$H + e^- = H^-$$

$$H_2 + e^- = H_2^-$$

$$OH + e^- = OH^-$$

$$HS + e^- = HS^-$$

$$Cl + e^- = Cl^-$$

$$Br + e^- = Br^-$$

Formation of anions decreases the chemical equilibrium abundance of electrons produced by ionization of monatomic H, another consequence of LeChatelier's Principle.

4. "Inert" elements – No net effect on electron abundance

(a) Noble gases – These are unimportant because of their high ionization potential (He, Ne, Ar, Kr) or low abundance (Xe).

(b) Carbon – No major electron sources or sinks, dilution of H gases is main effect

(b) Phosphorus – No significant electron sources or sinks

(c) Fluorine – HF bond too strong for significant F and F- production

(d) All others – Combination of high ionization potential and/or low abundance

Details are in the rest of this report and the attached figures and spreadsheet.

Methods

Ideal gas chemical equilibrium calculations were done along the Jovian adiabat of Hubbard & Militzer (2016 ApJ 820(1), 80) using the CONDOR code described by Fegley & Lodders (1994). Runs were done with the protosolar elemental abundances of Lodders (2003) and with variable abundances of selected elements either enriched or depleted relative to the protosolar composition.

Results – Ideal gas

I did several sets of gas phase chemical equilibrium calculations using a top down approach – starting with the condensate depleted gas at the top of the atmosphere and gradually adding one or more elements at a time to identify key reactions that are sources or sinks of electrons. I also did separate sets of runs where condensate cloud

formation was included (NH_3, H_2O, NH_4SH). Photochemical depletion of CH_4 is modeled by calculations for H + noble gases without any other volatiles.

H – He. Thermal ionization in the protosolar H – He mixture (91.209% H, 8.791% He by atoms) gives electron mole fractions of 8.6×10^{-10} (3993 K) to 9.4×10^{-227} (128.4 K). The major source of electrons and protons is the reaction

$$H = H^+ + e^-$$

A secondary source is the reaction

$$H_2 = H_2^+ + e^-$$

The major sink for protons is

$$H_2 + H^+ = H_3^+$$

The two major sinks for electrons are

$$H + e^- = H^-$$

$$H_2 + e^- = H_2^-$$

The calculated mole fraction and number density of electrons are in columns E and H of the spreadsheet entitled "Ionization summary" and Figure 1 shows log X(e-) along the entire adiabat. The black line is the solar composition H – He mixture.

H – He + (Ne, Ar, Kr, Xe). These calculations are for solar metallicity. The addition of the other noble gases changes the mass balance at constant total pressure because the mole fractions of H_2, He, H are very slightly smaller. For H + He, the mass balance can be written as the mole fraction sum

$$X_{H_2} + X_{He} + X_H + \cdots = 1$$

The ⋯ denotes the mole fractions of all the less abundant gases. However, when the other noble gases are also considered the mole fraction sum becomes

$$X_{H_2} + X_{He} + X_H + X_{Ne} + X_{Ar} + X_{Kr} + X_{Xe} + \cdots = 1$$

The ratio of the (Ne + Ar + Kr + Xe) protosolar abundances to that of H_2 + He is ~ 0.00016. Thus, the H_2 and He abundances are decreased to ~ 0.99984 times those in the H – He runs. The H mole fraction is ~ $(0.99984)^{1/2}$ times smaller because 2 H are produced by dissociation of H_2 gas. This gives a very slightly smaller electron mole fraction by about 4 parts in 100,000. The effect of the added noble gases is indirect via mass balance and there are no new electron sinks or sources. This mass balance effect occurs with each added element but is only noticeable for the more abundant elements (O, C, N, Ne, …) because of the overwhelming abundance of hydrogen. This is true even for the 3× solar elemental abundance models.

H + noble gases + C. The addition of carbon gives slightly lower electron mole fractions for two reasons. First, mole fractions of H – bearing gases + noble gases are diluted by addition of C. Second, formation of CH, CH_2, CH_3, CH_4, and other CH – bearing gases reduces the amount of hydrogen present as H_2. This gives less H from thermal dissociation of H_2, and less H^+ and e^- from ionization of H. Once again there are no new electron sinks or sources. The electron abundance from ionization of C, C_2, CH is insignificant compared to that from H, e.g., at ~ 3993 K (the highest T point on the adiabat) the abundance ratio is

$$\frac{C^+ + CH^+ + C_2^+}{H^+ + H_2^+ + H_3^+} \sim \frac{CH^+}{H_3^+} = 2.9 \times 10^{-8}$$

Column K in the spreadsheet is the ratio of the electron mole fraction with noble gases + C to the results for H – He. This ratio ranges from 0.9993 to 0.9998; the electron mole fraction is about 2 – 7 parts per 10,000 smaller than for H – He alone.

(H + noble gases + C) + N. This case is denoted prior + N and my description of subsequent runs uses the same nomenclature. The addition of nitrogen dramatically increases the electron abundance at all temperatures, e.g., by many orders of magnitude as temperature decreases (Figure 2 and spreadsheet columns M & N). Ammonia acts as a proton sink via the reaction

$$NH_3 + H^+ = NH_4^+$$

This alters the equilibrium abundance of H^+ from that due to hydrogen reaction network described in the H – He section. However, the equilibrium constant K_1 for H ionization is constant at a given temperature, and thus the electron and H abundances must change to re-establish equality of K_1 and the equilibrium quotient

$$K_1 = \frac{H^+ e^-}{H}$$

(The H^+, e^-, and H denote their respective partial pressures).

Hydrogen ionization accounts for most of the electrons and ionization of N – bearing gases is insignificant in comparison, e.g., at 3993 K we have

$$\frac{N^+ + N_2^+ + NH^+ + CN^+}{H^+ + H_2^+ + H_3^+} \sim \frac{NH^+}{H_3^+} = 2.9 \times 10^{-9}$$

Ammonia cloud condensation. I now consider condensation of NH_3 clouds and its effect on the electron abundance (spreadsheet columns P & Q). There is no effect until NH_3 clouds form. This occurs at T = 144.58 K, P = 0.65 bar for solar metallicity and immediately reduces the electron abundance because less NH_3 is available to react with protons. At 128.4 K, the lowest T point on the adiabat, the electron abundance is ~ 16% of that for the case where all NH_3 stays in the gas and $X(e^-)$ is ~ 2.5×10^{-145}, which is still > 81 orders of magnitude larger than for H – He.

Prior + O. The effect of oxygen is more complicated (spreadsheet columns S – W). The three major effects are (1) production of H_3O^+, (2) production of OH^-, and (3) dilution of the hydrogen mole fraction by addition of O and OH – bearing gases. At high temperatures oxygen leads to more ionization because H_2O is a good proton acceptor:

$$H_2O + H^+ = H_3O^+(hydronium)$$

For example, at 3993 K, the abundances of H_3O+, H_3+, and NH_4+ are about the same:

$$\frac{H_3O^+}{H_3^+} \sim 1.14 \qquad \frac{H_3O^+}{NH_4^+} \sim 0.51$$

Production of H_3O^+ alters the H^+ equilibrium abundance from the hydrogen reaction network and more H must ionize to keep the equilibrium quotient at the same value as the equilibrium constant K_1 for ionization of H gas. But this is a secondary effect only important at the highest temperatures because NH_4^+ is always more abundant than H_3O+ and the NH_4^+/H_3O^+ ratio increases strongly with decreasing temperature.

The formation of OH^-, which is an electron sink, also becomes more important with decreasing temperature

$$OH + e^- = OH^-$$

The importance of H_3O^+ decreases and of OH^- increases until at T ~ 1278 K their abundances are equal. The electron sink provided by OH^- formation is more important at lower temperature and the electron abundance is slightly less than that without oxygen (compare spreadsheet columns S & T). However, none of the oxygen gases ionize and produce significant amounts of electrons, e.g., via the reaction

$$H_2O = H_2O^+ + e^-$$

This is completely unimportant and the H_2O^+/e^- ratio is << unity, e.g., at 3993 K

$$\frac{H_2O^+}{e^-} \sim 3.8 \times 10^{-4}$$

Hydrogen gases remain the major source of electrons although the equilibria are strongly perturbed by the NH_4^+ and H_3O^+ ions.

Water cloud condensation. Columns V & W in the spreadsheet show the effect of water ice condensation, which starts at ~ 265 K. The electron abundance increases by ~ 7 parts in 10,000 as water (and thus OH^-) is removed by condensation. The subsequent condensation of the NH_3 ice cloud has a much larger effect (see above).

Prior + S. Addition of sulfur decreases the electron abundance at all temperatures (spreadsheet columns Y & Z). The decrease is ~0.9995 at 3993 K to 6.4×10^{-13} times at 128.4 K. This is due to formation of HS^- via

$$HS + e^- = HS^-$$

The electron affinity of HS is ~ 2.31 eV, about 0.49 eV larger than that of OH. The electron affinity of HS is also larger than that of other sulfur gases (S 2.08 eV, S_2 1.67 eV, SO 1.12 eV) and HS^- is the major S-bearing anion in the gas. No significant number of electrons are produced by sulfur gases; at 3993 K

$$\frac{S^+}{H_3^+} \sim 4.5 \times 10^{-7}$$

NH_4SH cloud condensation. This occurs at ~ 209 K for solar metallicity and leads to immediate increases in the electron abundance as H_2S is removed from the gas. The electron abundance is ~ 9% larger at the NH_4SH cloud base and ~ 47,300 times larger at ~ 145 K where the NH_3 ice cloud forms.

Prior + P. Spreadsheet columns AE & AF show this case. The electron abundance is identical to that without phosphorus at all temperatures. The major P cation is P^+ but it is insignificant, e.g., at 3993 K

$$\frac{P^+}{H_3^+} \sim 2.4 \times 10^{-8}$$

Likewise, none of the P-bearing anions are significant sinks for electrons. The most abundant anion is PH_2^- and at 3993 K

$$\frac{PH_2^-}{H^-} \sim 1.2 \times 10^{-4}$$

Prior + Cl. Columns AH – AK in the spreadsheet show this case. The major effect of Cl is as an electron sink because Cl has a large electron affinity (~ 3.613 eV) and formation of Cl^- is a major sink for electrons

$$Cl + e^- = Cl^-$$

Runs were made with and without P (spreadsheet columns AM – AO). These also showed no effect of P on the electron abundance, and it was excluded from all future runs to simplify the calculations. From this point on all runs exclude phosphorus.

Prior + F. This case is in columns AQ – AS of the spreadsheet. Fluorine does not alter the electron abundance because the F^- abundance is too small to be a significant sink for electrons. Monatomic F has a high electron affinity (~ 3.40 eV), but its concentration is extremely low because of the strong HF bond. For example, at 3993 K,

$$\frac{F^-}{Cl^-} \sim 3.0 \times 10^{-3}$$

This ratio becomes smaller with decreasing temperature and Cl^- is many orders of magnitude more abundant.

Prior + Br. This case is in columns AU – AW of the spreadsheet. Bromine reduces the electron abundance via formation of Br^-

$$Br + e^- = Br^-$$

This reaction becomes more important with decreasing temperature because of the weak HBr bond. The Br^- ion exceeds the abundance of other anions at 2194 K (H_2^-), 2044 K (OH^-), 1721 K (H^-), e^- (1244 K), 1098 K (HS^-), and 785 K (Cl^-). In the absence of alkali, alkaline earth, or ammonium bromide condensation, Br^- is the major anion below 785 K. Condensation reactions reduce the abundance of gaseous Cl and Br leading to HS^- being the dominant anion.

Prior + Na. If sodium is the only alkali metal present, it becomes the major electron source because of its low ionization potential (columns AY – AZ of spreadsheet). The larger electron pressure (at constant temperature) drives electron attachment reactions toward the anions (H^-, H_2^-, OH^-, HS^-). Conversely, sodium reduces the abundances of fluoride, chloride, and bromide ions in the gas phase by sequestering F, Cl, and Br into sodium halide gases, e.g., via the net thermochemical reactions

$$Na + F = NaF$$

$$Na + Cl = NaCl$$

$$Na + Br = NaBr$$

Competition between electron attachment equilibria and alkali halide formation is different for each halogen and leads to temperature – dependent peaks in the anion abundances. For example, the Br^- abundance peaks at ~ 1800 K and then decreases steadily with decreasing temperature. The Cl^- abundance peaks at ~ 1585 K. In contrast NaOH formation cannot compete with OH^- formation and the OH^- abundance increases

with decreasing temperature. However, this gradient is steeper at higher temperature and has an inflection at ~ 861 K where the total anion abundance (relative to that without Na) peaks.

Potassium and the other alkalis have similar effects; formation of alkali halide gases reduces the monatomic F, Cl, and Br abundances and reduces their importance as sinks for electrons.

Prior + K, Li, Rb, Cs. Potassium ionization is either the 1st (T < 3406 K) or 2nd (very highest T > 3406 K) most important source of electrons. Lithium is unimportant and the electron abundance is identical to that with K, at least to 3 decimal places. Over the range where it is in the gas (T > 830 K) Rb provides < 1% more electrons than the prior runs with K. Cesium provides < 1% more electrons than K at temperatures > 746 K. Spreadsheet columns BB – BL summarize results for K, Li, Rb, Cs.

Solar Metallicity. Columns BN – BO of the spreadsheet show this case, which has ~ 9% more electrons than the prior case with all alkalis. This ratio is larger at lower temperatures, but is physically unreal because most of the other elements condensed out of the gas at much higher temperatures > 2000 K.

Enhanced Metallicity. Columns BQ – BS of the spreadsheet show this case, which is 3× solar metallicity (all elements). The electron abundance at high temperatures is ~ 1.7× that for the solar metallicity case. This is almost equal to the square root of 3 and is consistent with a large fraction of electrons coming from heavy elements (Na, K), which are enriched three times solar.

Comparison of Ideal Gas Ionization Computations with Published Results

I did two comparisons of my calculations with published work on ionization of high T, high P gases. One comparison is to the results of Hilsenrath & Klein (1965) and Gilmore (1955, 1959, 1967) on air heated to high T and P. The second comparison is to the results of Patch (1969) for hydrogen heated to high T and P.

Dry Air –Gilmore (1955, 1959, 1967) and Hilsenrath & Klein (1965) calculated the equilibrium composition of dry air at high pressure and temperature. Figure 3 (DryAir.spw) compares my ideal gas calculations with the real gas calculations of Hilsenrath & Klein (1965) and the ideal gas calculations of Gilmore (1955) along the 6000 K isotherm. The comparison looks good until a density of 0.565 g/cm^3 where divergence occurs. For reference, the calculations presented in this work go up to 0.305 g/cm^3 at ~ 3993 K, 158 kbar on the Hubbard-Militzer Jupiter adiabat.

Hilsenrath & Klein do not tabulate their results at higher densities but the shape of the ideal gas curve shows the disagreement will increase with increasing density. The major disagreement between my results and the prior work is due to singly ionized molecular oxygen (O_2^-) for which thermodynamic data have changed since publication of the earlier calculations. At 2000 K the ideal gas calculations that exclude O_2^- almost exactly reproduce Hilsenrath & Klein up to their highest density tabulated values. The key point is that their data for this species makes it much less abundant than the currently accepted data I am using. Thus, when I include O_2^- in my calculations it soaks up almost all available electrons via the reaction

$$O_2 + e^- = O_2^-$$

Taking the comparison at face value the highest density point, which is log (ρ/ρo) = 2.4 (absolute air density of 0.32 g/cm^3), disagrees. At 6000 K whether O_2^- is present or absent does not change things that much at all because the major anion is singly ionized monatomic oxygen (O^-). The thermodynamic data used by Hilsenrath & Klein (1965) for this gas are much closer to the currently accepted data and there is about a factor of two difference in the O^- mole fraction between the two sets of calculations. So, it is unclear whether or not real gas corrections are needed at 6000 K for dry air either. The bottom line is that the ideal gas calculations reproduce the real gas calculations done by Hilsenrath & Klein (1965) up to at least ρ ~ 0.3 g/cm^3 at 2000 K and up to ~ 0.565 g/cm^3 at 6000 K.

Hydrogen – Patch (1969) published ideal gas calculations with Coulomb interactions between charged particles but no virial corrections.

Hydrogen at 4000 K and 1 Atmosphere

Gas	Patch	IVTAN	CONDOR
H_2	0.2334	0.2337	0.2337
H	0.7666	0.7663	0.7663
e-	4.814×10^{-8}	4.674×10^{-8}	4.676×10^{-8}
H-	2.60×10^{-10}	2.40×10^{-10}	2.40×10^{-10}
H_3^+	8.66×10^{-9}	6.04×10^{-9}	6.07×10^{-9}
H_2^+	7.97×10^{-10}	8.14×10^{-10}	8.20×10^{-10}
H^+	3.90×10^{-8}	4.01×10^{-8}	4.01×10^{-8}

The table above summarizes comparisons to his work with the CONDOR (mass balance – mass action) and IVTAN (Gibbs energy minimization) ideal gas codes at 4000 K and 1 atmosphere pressure. The major difference is the larger abundance of H_3^+ (shown in red). This is consistent with Patch's statement that: "The largest possible sources of inaccuracy in this study were the constants and potential for H_3^+ which were used to calculate the partition function. These quantities were based on Conroy's (1964) *ab initio* calculations, which are believed reliable. However, there are no experimental vibration frequencies or dissociation energy for H_3^+." Patch (1969) used the H_3^+ dissociation energy from Patch (1968). This is 13.6 kJ larger than that of Gurvich et al (1989) used here:

$$H_3^+ = H + H + H^+$$

$$D_0^o = 869.77\ kJ\ mol^{-1}\ \text{(Patch 1968)}$$

$$D_0^o = 856.16\ kJ\ mol^{-1}\ \text{(Gurvich et al 1989)}$$

The H_3^+ ion forms via the reaction

$$H_2 + H^+ = H_3^+$$

This decreases the abundance of protons, which perturbs other equilibria involving neutral and charged hydrogen species, e.g.,

$$H = H^+ + e^-$$

More H must ionize to restore equilibrium and the e- abundance also increases.

This can be seen in the table below, which compares electron mole fractions computed by Patch and from the IVTAN and CONDOR codes at 4000 K and variable pressure.

Electron Mole Fraction at 4000 K and Variable Total Pressure

X(e-) at P/atm	1	10	100	1,000
Patch	4.814×10^{-8}	2.536×10^{-8}	1.641×10^{-8}	9.020×10^{-9}
IVTAN	4.674×10^{-8}	2.166×10^{-8}	1.356×10^{-8}	7.420×10^{-9}
CONDOR	4.676×10^{-8}	2.170×10^{-8}	1.360×10^{-8}	7.439×10^{-9}

The differences between the Patch's (1969) electron abundances and those computed here increase with increasing pressure up to 100 atmospheres and then level off (3.0% – 1 atm, 17% – 10 atm, 20.7% – 100 atm, and 21.2% – 1000 atm). These differences are about the same size as those found for other species at the same pressures and are plausibly due to his H_3^+ data, which affects the abundances of other species via the coupled equilibria. Alternatively, the differences could be due to Coulomb interactions. However, if Coulomb interactions were important their effect would be ~ a factor of 5× larger from 1 – 1000 atmospheres according to Eq (1) of Patch (1969) while the differences in the abundances of electrons, H_3^+, H^-, H^+, and H_2^+ are ~ the same size and vary by 10 – 20 % over the same range.

Real Gas Corrections

Corrections for intermolecular forces between neutral gas atoms and molecules in a gas become significant as the gas density approaches that of the liquid and the ideal gas equation no longer applies. The P – T - ρ data for the Jovian adiabat show it reaches 0.3048 g/cm^3 at ~ 3993 K, 158 kbar. This is about 10 × the density of H_2 at its critical point and about a third of the density of liquid water at ambient pressure. Thus, the gas is highly non-ideal and liquid-like at the highest P, T on the model adiabat. The

compression factor Z quantifies the non-ideality and it is the ratio of the PV_m product or the P/ρ_m quotient (where V_m = molar volume, and $\rho_m = 1/V_m$ = molar density) to RT:

$$Z = \frac{PV_m}{RT} = \frac{1}{RT} \cdot \frac{P}{\rho_m}$$

Z is unity for an ideal gas (i.e., with attractive and repulsive forces in balance), is greater than unity for an incompressible real gas (repulsive forces are dominant) and is less than unity for a highly compressible real gas (attractive forces are dominant). A compression factor > unity – the case along the Jupiter adiabat – arises because repulsive forces are dominant and consequently fugacity (f) > pressure (P), and the fugacity coefficients (ϕ) are also > unity. Figure 4 (H2HeVirl.spw) shows the compression factor Z along the adiabat. The P – T - ρ data for the Jovian adiabat combined with an assumed mean molecular weight give curve HM (Hubbard-Militzer). This shows Z ~ 1 for T ≤ 400 K, Z ≤ 2 until ~ 2900 K and increasing non-ideality until Z reaches ~ 3.7 at ~ 4000 K. (I compute the same curve for Z using either μ = 2.40 for H_2 – He + 3× solar CH_4, NH_3, H_2O or 2.34 for a solar H_2 – He mixture.)

Fugacity Coefficients

Non-ideality effects on chemical equilibria can be computed using fugacity coefficients (ϕ) as a function of P, T, and composition for each gas. This can be done using –

(a) the virial equation of state (Hirschfelder et al 1964)

$$\frac{PV_m}{RT} = Z = 1 + \frac{B}{V_m} + \frac{C}{V_m^2} + \frac{D}{V_m^3} + \frac{E}{V_m^4} + \cdots$$

(b) an empirical EOS such as the van der Waals equation,

$$Z = 1 + \left(b - \frac{a}{RT}\right)\frac{1}{V_m} + \left(\frac{b}{V_m}\right)^2$$

other empirical cubic EOS such as the Redlich – Kwong equation or the Peng – Robinson equation (e.g., Bakker 2012, Peng & Robinson 1976),

(c) a fundamental EOS giving all properties of a gas in terms of its Helmholtz energy (Span & Wagner 1997), or

(d) van der Waals' corresponding states theory and reduced variables, i.e., ratios to critical parameters

$$\text{reduced temperature: } T_R = \frac{T}{T_C}$$

$$\text{reduced pressure: } P_R = \frac{P}{P_C}$$

$$\text{reduced volume: } V_R = \frac{V}{V_C}$$

$$\text{reduced compression factor: } Z_R = \frac{P_C V_C}{R T_C}$$

Fegley and Prinn (1986) used the reduced variable approach to compute non-ideal gas equilibria in the atmosphere of Uranus. Kite et al (2020) used the virial EOS and compared it to the hydrogen EOS of Saumon et al (1995). Appendix C of Kite et al (2020) describes computation of and tabulates the second, third, and fourth virial coefficients for H_2; a similar approach can be used for helium.

List of Figures

Figure 1. Chemical equilibrium abundances of electrons along the model Jupiter adiabat. The mole fraction of electrons is plotted.

Figure 2. The same as in Figure 1 but comparing the chemical equilibrium abundances of electrons for a H – He solar composition mixture (black curve) and a H – He – C – N –

noble gas mixture (red curve). See the text and spreadsheet "Ionization Summary" for details.

Figure 3. Comparison of ideal gas and real gas chemical equilibrium calculations for dry air along the 6000 K isotherm. See text for details.

Figure 4. The compression factor Z along the model Jupiter adiabat. See text for details.

References

Bakker, R.J. 2012 Thermodynamic properties and applications of modified van der Waals equations of state. pp. 163-190, Chapter 7 in Thermodynamics – Fundamentals and its Applications in Science, ed. R. Morales-Rodriguez, Intech.

Fegley, B., Jr. 2013 *Practical Chemical Thermodynamics for Geoscientists*, Academic Press/Elsevier, 698 pages.

Fegley, B., Jr. and Lodders, K. 1994 Chemical Models of the Deep Atmospheres of Jupiter and Saturn. *Icarus* **110**, 117-154.

Fegley, B., Jr. and Prinn, R. G. 1986. Chemical Models of the Deep Atmosphere of Uranus. *Astrophys. J.* **307**, 852-865.

Gilmore, F.R. 1955 Equilibrium Composition and Thermodynamic Properties of Air to 24,000 °K. RAND Research Memorandum RM-1543.

Gilmore, F.R. 1959 Additional Values for the Equilibrium Composition and Thermodynamic Properties of Air. RAND Research Memorandum RM-2328.

Gilmore, F.R. 1967 The Equilibrium Properties of High Temperature Air. Vol 1 of Thermal Radiation Phenomena DASA-1971-1, eds. J.L. Magee & H. Aroeste.

Gurvich, L.V., Veyts, I.V., & Alcock, C.B. 1989 Thermodynamic Properties of Individual Substances vol 1 part 1, 4th ed.

Hilsenrath, J. & Klein, M. 1965 Tables of Thermodynamic Properties of Air in Chemical Equilibrium Including Second Virial Corrections from 1500°K to 15,000°K. Report AEDC-TR-65-58, Arnold Engineering Development Center, Arnold Air Force Station, TN.

Hirschfelder, J.O., Curtiss, C.F. & Bird, R.B. 1964 Molecular Theory of Gases and Liquids, corrected printing with notes added, John Wiley, NY.

Kite, E.S., Fegley, B. Jr., Schaefer, L., Ford, E.B. (2020) Atmosphere origins for exoplanet sub-Neptunes. ApJ, 891:111 (16 pp) 2020 March 10.

Lodders, K. 1999. Alkali element chemistry in cool stellar dwarf atmospheres. Astrophys. J. 519(2), 793-801.

Lodders, K. 2003. Solar system abundances and condensation temperatures of the elements. Astrophys. J. 591(2) 1220-1247.

Patch, R.W. 1969 Absorption coefficients for hydrogen I. Composition. JQSRT 9, 63-87.

Patch, R.W. 1968 Partition functions of the ground electronic states of H_3^+ and H_2^+. J. Chem. Phys. 49, 961-962.

Peng, D.Y. & Robinson, D.B. 1976 A new two-constant equation of state. Ind Eng Chem Fund 15(1), 59-64.

Saumon, D., Chabrier, G., and van Horn, H. M. 1995. An equation of state for low-mass stars and giant planets. Astrophys J. Suppl. 99, 713-741.

Span R., Wagner W. 1997 On the extrapolation behavior of empirical equations of state. Int J Thermophys 18, 1415-1443

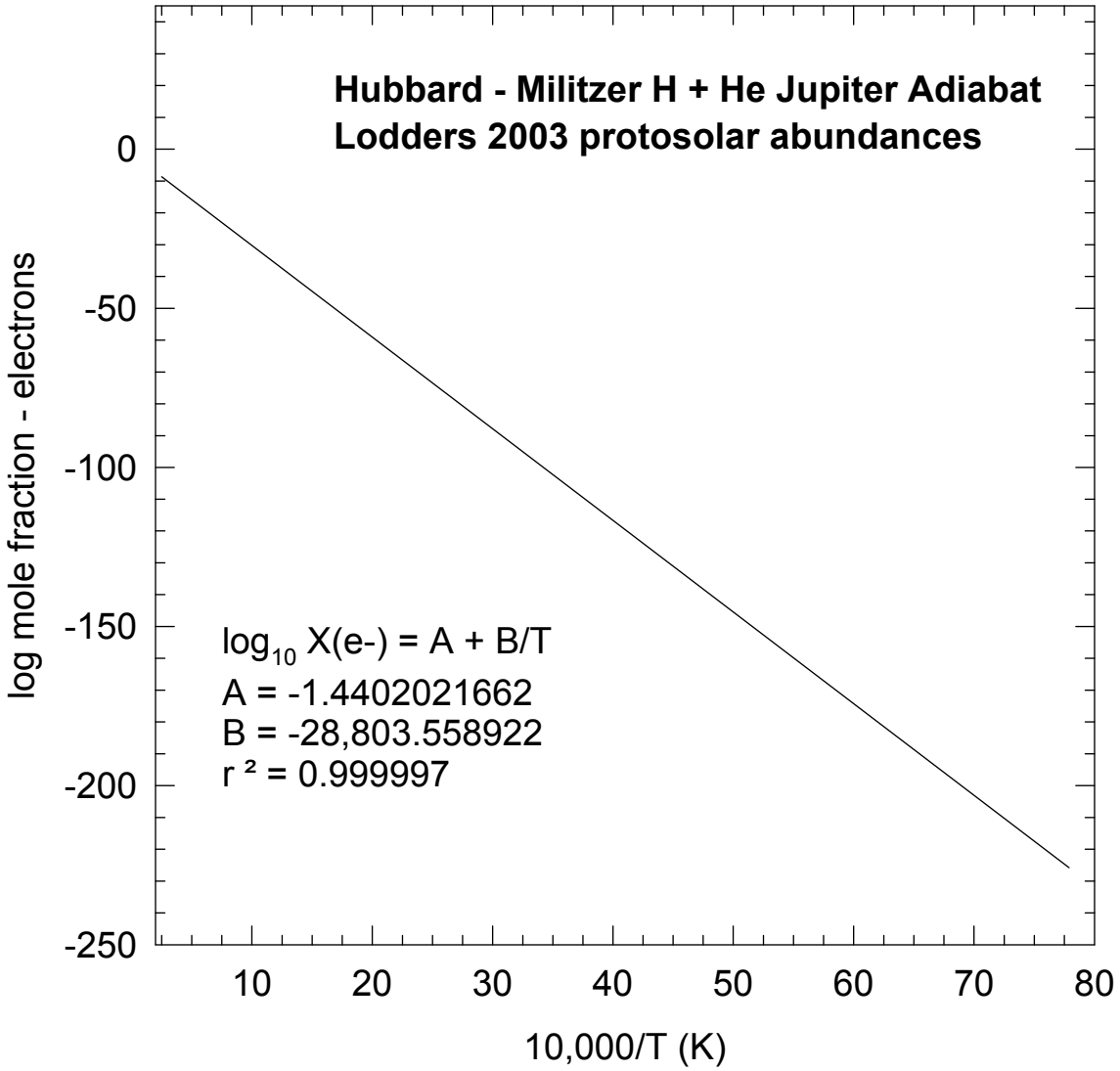
Hubbard - Militzer H + He Jupiter Adiabat
Lodders 2003 protosolar abundances
log mole fraction - electrons
0
-50
-100
-150
-200
-250
10
20
30
40
50
60
70
80
10,000/T (K)
log10 X(e-) = A + B/T
A = -1.4402021662
B = -28,803.558922
r ² = 0.999997

H2Heion.spw

solar H-He mixture
$\log_{10}$ X(e-) = A + B/T
A = -1.4402021662
B = -28,803.558922
r ² = 0.999997

solar mix H+noble+c+N
$\log_{10}$ X(e-) = A + B/T
A = -3.9993649084
B = -17,914.592436
r ²= 0.999993

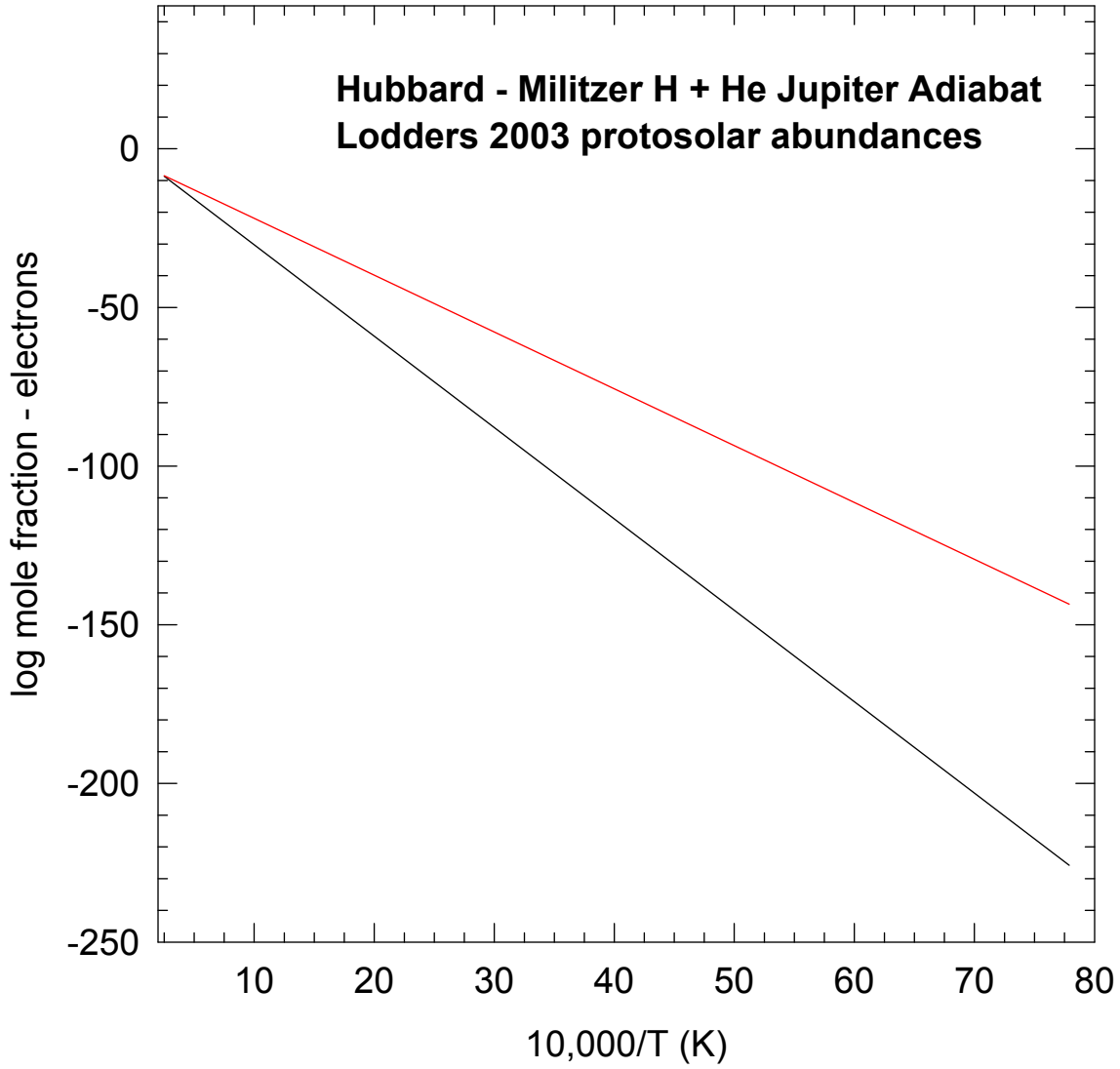

H2Heion.spw

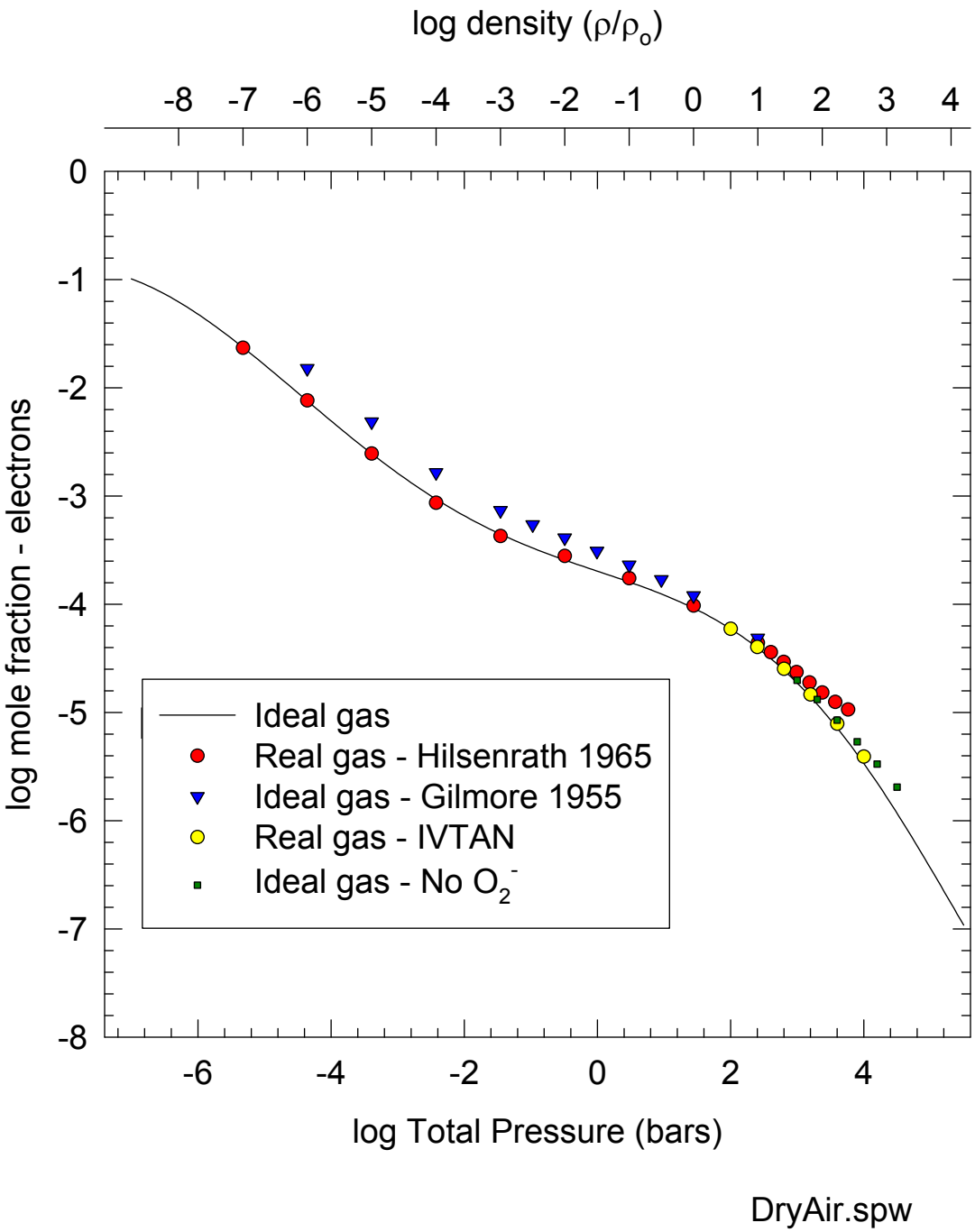
log density (ρ/ρo)
-8 -7 -6 -5 -4 -3 -2 -1 0 1 2 3 4
0 -1 -2 -3 -4 -5 -6 -7 -8
log mole fraction - electrons
Ideal gas
Real gas - Hilsenrath 1965
Ideal gas - Gilmore 1955
Real gas - IVTAN
Ideal gas - No O2-
-6 -4 -2 0 2 4
log Total Pressure (bars)
DryAir.spw

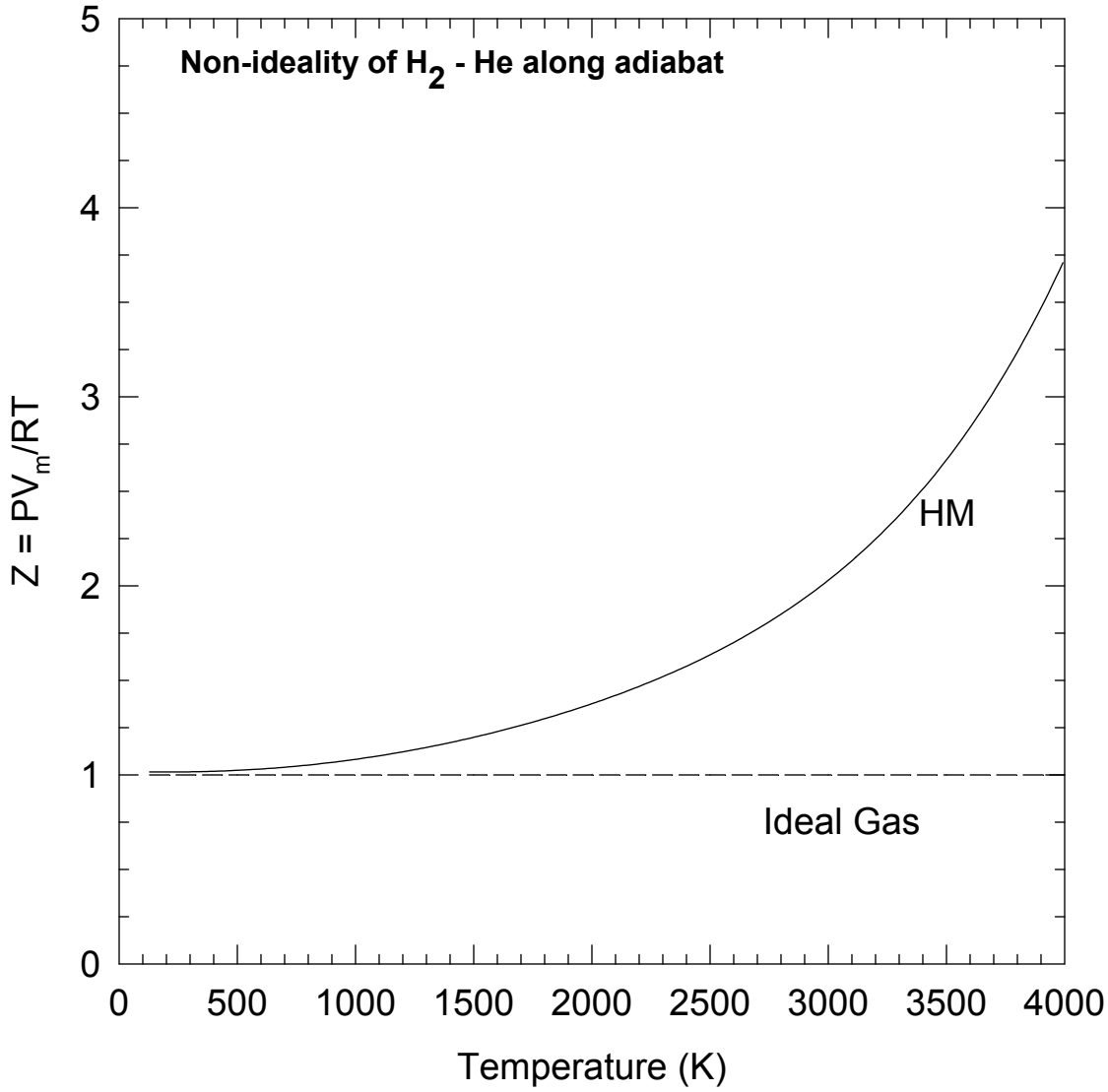

H2HeVirl.spw